ACS OMEGA

http://pubs.acs.org/journal/acsodf

Article

Highly Stretchable and Self-Adhesive Elastomers Based on Polymer Chain Rearrangement for High-Performance Strain Sensors

Cunguang Lou,[⊥] Enjie Liu,[⊥] Tong Cheng, Jun Li, Hongzan Song, Guangwei Fan, Lei Huang, Bin Dong,* and Xiuling Liu*

Cite This: *ACS Omega* 2022, 7, 5825−5835

Read Online

ACCESS | Metrics & More | Article Recommendations | Supporting Information

ABSTRACT: Polydimethylsiloxane (PDMS) has been widely used in many fields. However, the polymerization process of the siloxane chain is highly complex, and it is challenging to enhance the mechanical properties of PDMS elastomers significantly. We found that adding a small amount of polyoxyethylene lauryl ether (Brij-35) into siloxane polymers can result in B-PDMS elastomers with high tensile properties and strong adhesion. It is worth noting that this is the first study to improve the mechanical properties of PDMS using Brij-35. Here, we intensely studied a variety of process conditions that influence the cross-linking of PDMS, emphasizing the modification mechanism of the polymer chain. The hydroxyl groups in Brij-35 and the platinum catalyst in PDMS form a complex, which inhibits the cross-linking process of PDMS, not only forming a heterogeneous cross-linking network in the B-PDMS but also disentangling the strongly wound siloxane polymer chain, thereby rearranging the PDMS polymer chains. Furthermore, in order to prepare a strain sensor based on the B-PDMS elastomer under safe and convenient conditions, we prepared laser-scribed graphene powder (LSGP) by laser-scribing of graphene oxide (GO) films, and the LSGP and carbon nanotubes (CNTs) endowed the B-PDMS elastomers with excellent electrical properties. The sensor could firmly adhere to the skin and generate a high-quality response to a variety of human motions, and it could drive the robotic hand to grasp and lift objects accurately. The high-performance strain sensors based on B-PDMS have broad applications in medical sensing and biopotential measurement.

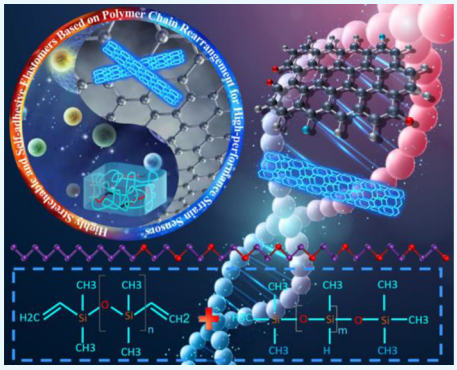

1. INTRODUCTION

Artificial electronic skin (e-Skin) is an electronic sensor that can simulate human skin's basic perception by responding to changes in resistance or capacitance while maintaining key features such as low thickness, extensibility, and compliance. Because of these characteristics, the e-Skin has great potential applications to be used in intelligent robots, human-computer interactions, motion detection, and health monitoring.[1−4] The e-Skin could be connected to the human skin or organs without obvious discomfort and invasiveness; it has been used to detect a variety of biological signals that are closely related to personal health, such as physical exercise,[5,6] heart rate,[7,8] skin temperature,[5] breathing,[6] electrocardiogram,[9,10] and electroencephalogram.[11] Therefore, it is crucial to maintain good conformal contact between the elastomer and the skin to acquire biological signals accurately. If the adhesion between the elastomer and the skin surface is poor, it will introduce severe motion artifacts and interference signals when collecting physiological signals.

Polydimethylsiloxane (PDMS), as one of the widely used supporting materials of e-Skin, not only has the characteristics of thermosetting but also has excellent mechanical extensibility, high elasticity, biocompatibility, and environmental stability; it has been widely used in flexible circuits, drug-delivery carriers, superhydrophobic surfaces, microfluidic chips, and other fields.[12−16] However, ordinary PDMS elastomers could not meet the special demand of flexible electronic products, so it is necessary to synthesize elastomers with an excellent performance using a simple process. At present, many methods of synthesizing high-performance flexible, functional materials using PDMS have been reported.[17−21] Li et al. modified the silicone molecular chain by introducing an iron complex bond into the aminomethyl siloxane molecular chain, and the elastomer exhibited excellent ductility and self-healing.[22] Kang et al. carried out the condensation reaction with aminopropyl-terminated PDMS to form a tough and self-healing stretchable film.[1] Jeong et al. added ethoxylated polyethylenimine to the siloxane polymerization process, and the heterogeneous cross-linking network formed during the

Received: October 16, 2021
Accepted: January 24, 2022
Published: February 8, 2022

https://doi.org/10.1021/acsomega.1c05789
ACS Omega 2022, 7, 5825−5835

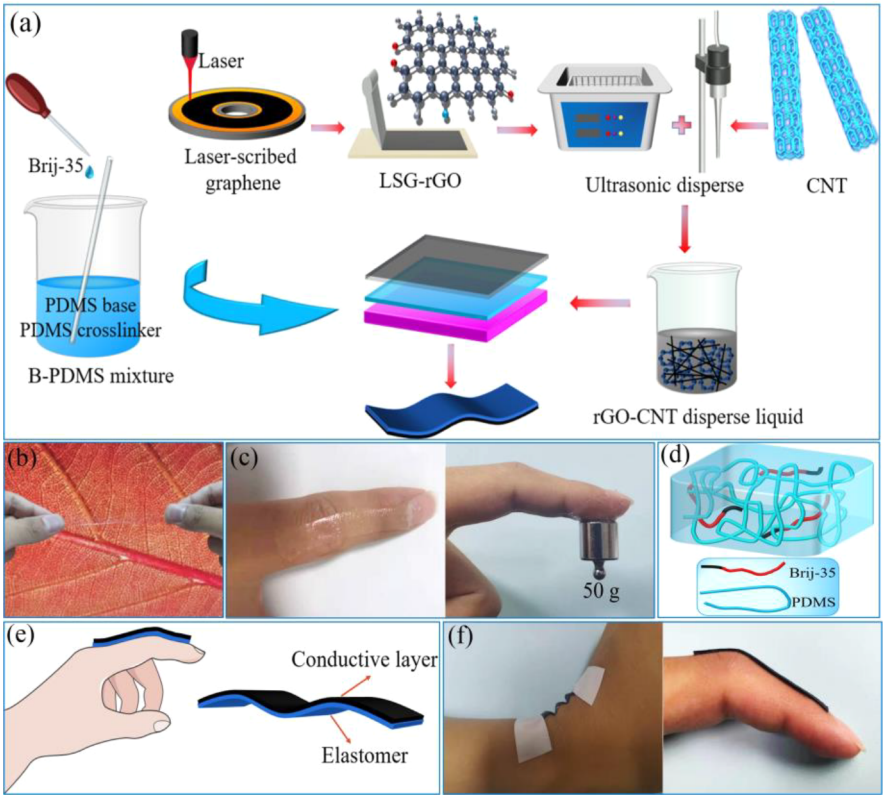

Figure 1. (a) Schematic diagram of the preparation process of the B-PDMS/rGO/CNT strain sensor. (b) Stretching B-PDMS elastomer. (c) Elastomer attached to the skin. (d) Structure schematic diagram of the elastomer. (e) Schematic diagram of a strain sensor with a top conductive layer and a bottom adhesive layer. (f) Strain sensors adhere to the skin.

cross-linking process changed the mechanical properties of the organosilicon polymer.[23] It has shown that the mechanical properties and the hydrophobicity of siloxane polymers can be effectively adjusted by redesigning the molecular chain or introducing other components. Polyoxyethylene lauryl ether (Brij-35) is a surfactant, commonly known as Brij-35, with a hydrophobic aliphatic group and a hydrophilic polyethylene glycol group.[24,25] Brij-35 has been widely used in surface modification, protein separation, and micellar solution.[26−28] For example, Squillace et al. investigated the surface modification of these molecular coatings by modifying the electrode and the conductive interface with Brij.[26]

In order to obtain high-quality physiological signals while maintaining conformal contact with the human skin, it is also necessary to integrate the conductive material into the elastomer to obtain excellent electrical properties. The combination of conductive materials and polymers using chemical or physical methods is common to obtain high-performance flexible sensors. Their operation mechanism is usually that its resistance or capacitance changes with the deformation of the sensor. Among them, rGO and carbon nanotubes (CNTs) are widely used to produce artificial electronic skin because of their high electrical conductivity, excellent mechanical properties, and easy processability.[29−32] For example, Pan et al. transferred three-dimensional (3D) graphene films prepared by chemical vapor deposition to PDMS and prepared a susceptible strain sensor.[33] Wang et al. added rGO and CNTs to highly stretchable polyurethane to collect high-quality physiological signals.[34] However, the synthesis method of rGO generally requires the treatment of graphene oxide (GO) using a chemical reduction process; the process is complex, time-consuming, toxic, and expensive, limiting its applications.[35] Recently, laser-induced graphene has attracted wide attention, providing a new idea for preparing high-performance rGO with convenient, easy, and safe handling. Lin et al. prepared porous graphene on polyimide films by CO_2 infrared laser.[36] Maher et al. obtained rGO by the laser-scribing of GO films using a LightScribe DVD burner called laser-scribed graphene (LSG).[37]

In this work, we designed a flexible strain sensor with adjustable mechanical properties and electrical properties. In order to enhance the mechanical properties of an ordinary PDMS elastomer, we added Brij-35 containing hydroxyl groups into PDMS, which changed the ultimate strain, Young's modulus, and the adhesion of PDMS in a simple way and obtained a B-PDMS elastomer with high stretchability and strong adhesion. The addition of Brij-35 to PDMS affects the hydrosilylation addition reaction, forming heterogeneous cross-linking networks and allowing the strongly wound siloxane polymer chains to be unentangled, thereby rearranging the polymer chains. Subsequently, in order to endow the elastomer with a wide sensing range and high sensitivity, we embedded rGO and CNTs as conductive networks into B-PDMS, in which laser-scribed graphene powder (LSGP) is prepared by laser-scribing the GO film, followed by harvesting graphene. The sensor can adhere to the human skin to generate high-quality signals to monitor human motion signals caused by joint or muscle activities. The primary significance of this study is (A) we innovatively modified PDMS with Brij-35, prepared a highly stretchable and self-adhesive elastomer, and deeply studied the reaction mechanism of Brij-35 on the mechanical properties of PDMS. It is worth noting that this is

https://doi.org/10.1021/acsomega.1c05789
ACS Omega 2022, 7, 5825−5835

the first study to improve the mechanical properties of PDMS by using Brij. (B) We have prepared LSGP by the laser-scribing technology, followed by harvesting graphene, which is the first research to prepare the strain sensor using LSGP. This preparation method makes the B-PDMS elastomer have greater advantages.

2. RESULTS AND DISCUSSION

The devices with sensing layers and adhesive layers can be used as conformal wearable strain sensors. In order to improve the mechanical properties of commercial PDMS, such as tensile properties and adhesion, we added Brij-35 to the mixture of the PDMS base and the cross-linking agent. The Brij can affect the hydrosilylation addition reaction of PDMS, and elastomers with different mechanical properties can be obtained by controlling the content of Brij in PDMS, curing temperature, and curing time. It is worth pointing out that this method makes PDMS exhibit excellent softness, scalability, and adhesion and further expands the application prospect of PDMS and Brij. In order to make the B-PDMS film useful as a strain sensor, the rGO/CNT dispersion is spray-coated on the adhesive layer after B-PDMS prepolymer curing, and the conductive layer and the adhesive layer can be firmly bonded. The preparation process of the B-PDMS elastomer and the B-PDMS/rGO/CNT strain sensor is shown in Figure 1a. Elastomers with high stretching and strong adhesion can maintain good conformal contact with the skin without slipping, delamination, or fracture even when joints move rapidly, which is of critical importance for collecting high-quality human physiological signals. The photographs of the prepared elastomer are shown in Figure 1b, c, and the microstructural diagram of the B-PDMS elastomer is shown in Figure 1d. The strain sensor has a top conductive layer and a bottom adhesive layer, the resistance of the conductive layer will change with stretching, and the insulating adhesive layer can prevent the skin from being electrically stimulated. The schematic diagram of the strain sensor is shown in Figure 1e, and the physical diagram of the sensor adhering to the skin is shown in Figure 1f.

2.1. B-PDMS Elastomer. The interior of PDMS contains many components; PDMS is generally divided into the base (polymer) and the cross-linking agent (curing agent). The mixture of the PDMS base and the cross-linking agent will solidify into an elastomer at a certain temperature for a period of time. We found that the B-PDMS elastomer with high stretchability and strong adhesion can be prepared by adding a small amount of Brij-35 in the cross-linking process of PDMS. So far, although some researchers have used PDMS and Brij to study surface properties such as surface hydrophobicity,[25−27] no one has used Brij to change the mechanical properties of PDMS. Many experiments on PDMS and Brij lack a theoretical basis. In order to study the factors affecting the mechanical properties of PDMS, the curing time under different Brij contents was examined, curing temperature was recorded, and they were named according to the preparation conditions, as shown in Table 1. Here, the ratio of the PDMS base to the cross-linking agent is 10:1, adding Brij-35 with a weight ratio of 0.5, 0.9, and 1.2% and curing B-PDMS at 50 °C (lower temperature) and 100 °C (higher temperature). It can be seen that PDMS is not only affected by the Brij content and curing temperature but also by the curing rate. At the same temperature, with the increase in the Brij-35 content, B-PDMS needs a longer curing time, that is, it corresponds to the slower curing rate. When the content of Brij is constant, the curing rate of PDMS will slow down with the decrease in the curing temperature. By adjusting the parameters in the preparation process, we studied the influence of Brij on the cross-linking process of PDMS. The elastic modulus, ultimate strain, adhesion, and other mechanical properties of elastomers prepared under different conditions were significantly different.

Table 1. Recorded Parameters in the Process of Preparing the Elastomer

elastomer name	wt% of Brij-35	temperature (°C)	curing time (h)
L-PDMS	0	50	2
B1-L-PDMS	0.5	50	8
B2-L-PDMS	0.9	50	18
B3-L-PDMS	1.2	50	27
H-PDMS	0	100	0.5
B1-H-PDMS	0.5	100	3
B2-H-PDMS	0.9	100	7
B3-H-PDMS	1.2	100	13

Reaction Mechanism of PDMS. The PDMS base and the curing agent are cross-linked under the action of the platinum catalyst after mixing, and vinyl-terminated polydimethylsiloxane and hydrogenated siloxane cross-linking agents undergo hydrosilylation addition reaction to form a closely entangled 3D silicone network,[38,39] some cross-linked polymers of which can be unentangled. The chemical structures of the PDMS base and the cross-linking agent are shown in Figure 2a, and the reaction mechanism is shown in Figure 2b. When the PDMS prepolymer is cured at a high temperature, the curing time is short, the high temperature initially increase the diffusivity and mobility of polymer chains, subsequently locking in entanglements rapidly without allowing for disentangling, so that the PDMS elastomer has a high elastic modulus and low limit strain. When the PDMS prepolymer is cured at a low temperature, the curing rate slows down, and the polymer chains are allowed to disentangle and release minute stresses, so that the elastomer has low elastic modulus and high ultimate strain.[40]

Modification Mechanism of PDMS. Because the PDMS addition reaction requires platinum atoms that can complex with vinyl in the PDMS base, substances that can complex platinum more effectively than vinyl groups may be used as cross-linking inhibitors,[40,41] such as Brij-35 with hydroxyl terminals. Brij-35 is an aliphatic compound composed of the hydrocarbon chain and the polyoxyethylene chain with a hydroxyl terminal,[42] as shown in Figure 2c. On the one hand, the hydroxyl group in Brij-35 and the Pt^{+} in platinum catalyst form a complex, which inhibited the cross-linking of PDMS and formed a heterogeneous cross-linking network with low cross-linking density, and some of the ends of the polymer chain were dangled.[23,43,44] On the other hand, with the diffusion of Brij-35 between polymer chains, the suppressed cross-linking process causes B-PDMS to require longer cure times, the slower curing rate causes the siloxane polymer chain to disentangle and release minute stresses,[40] the elastomer deforms with less energy, and the rearranged polymer chain makes the elastomer softer,[45−47] as shown in Figure 2d. These factors enhance the ultimate strain, flexibility, and adhesion of B-PDMS elastomers. In addition, the interaction between Brij and the platinum catalyst is weakened at a higher temperature so that Brij cannot effectively inhibit the cross-linking of PDMS.[43] Moreover, when PDMS is cured at a lower

https://doi.org/10.1021/acsomega.1c05789
ACS Omega 2022, 7, 5825−5835

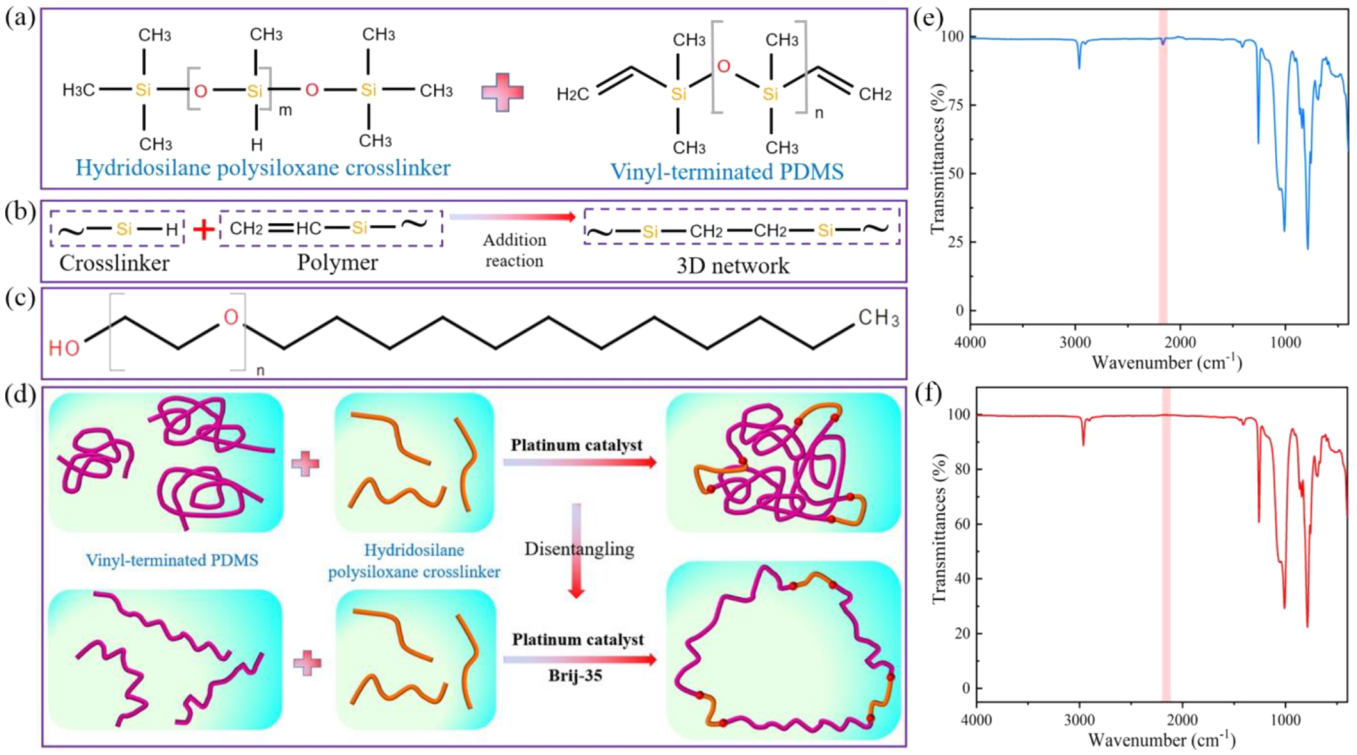

Figure 2. (a) Chemical structure of PDMS. (b) Cross-linking reaction of PDMS. (c) Chemical structure of Brij-35. (d) Schematic diagram of the disentanglement of the siloxane polymer chain. (e) FT-IR of B-PDMS before cross-linking. (f) FTIR of B-PDMS after cross-linking.

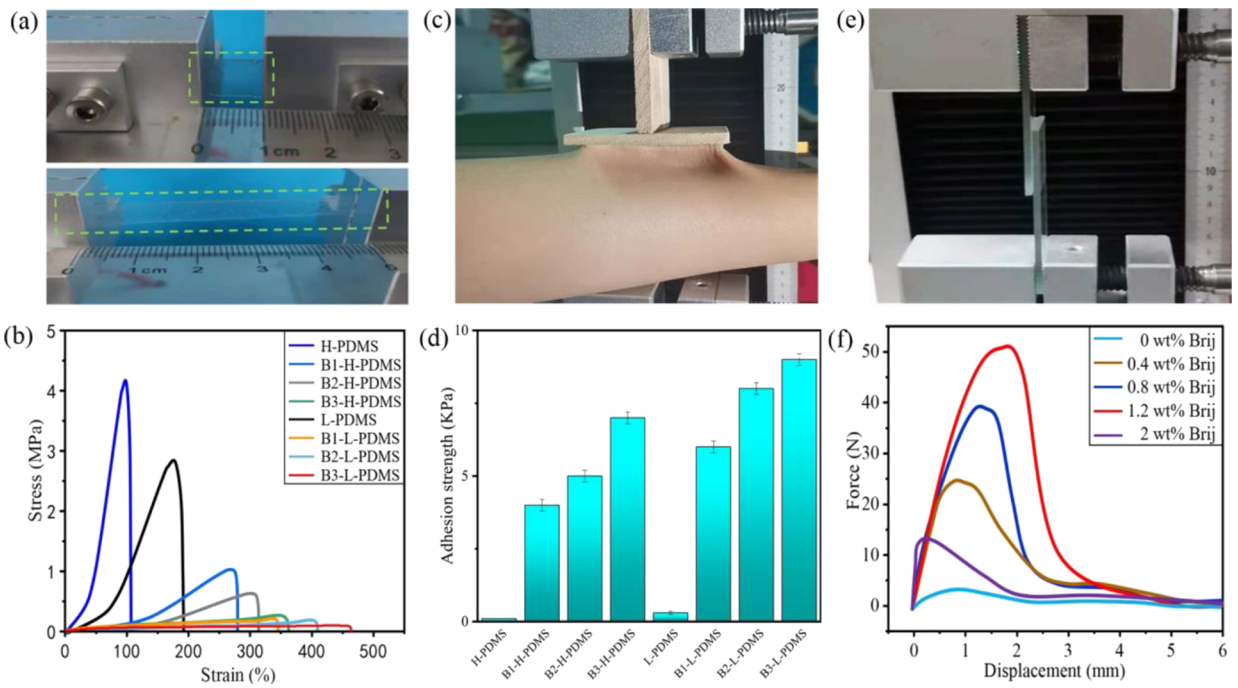

Figure 3. Mechanical properties of B-PDMS elastomers: (a) images of elastomers under original and tensile conditions. (b) Stress−strain curves of elastomers prepared under different conditions. (c) Photographs of B-PDMS elastomer adhesion test. (d) Testing of the adhesion of B-PDMS to the skin. (e) Photographs of the lap shear test. (f) Load−displacement curves of B-L-PDMS elastomers.

temperature, the mechanical properties of PDMS elastomers will change, and the slower curing rate will make the ultimate strain of PDMS elastomer higher.[48] However, excessive Brij will make it difficult for B-PDMS to get effective cross-linking, which will decrease the ultimate strain and adhesion strength of the elastomer. Therefore, in order to obtain elastomers with high extensibility and high adhesion, it is necessary to control the content of Brij, curing temperature, and curing rate.

Characterization of Elastomers. To further verify the difference in the cross-linked structure of the B-PDMS and PDMS, we carried out swelling experiments on elastomers. The PDMS elastomer and the B-PDMS elastomer were used

https://doi.org/10.1021/acsomega.1c05789
ACS Omega 2022, 7, 5825−5835

for the swelling experiment, and the weight change before and after swelling was measured by soaking in the xylene solvent for 5 days.[49] The swelling experiment is described in detail in the Supporting Information. Figure S1 (Supporting Information) compares the swelling rates of elastomers prepared under different conditions. It can be seen that the maximum swelling rate of the B-PDMS elastomer is 9.7, the swelling rate of the PDMS elastomer is 2.1, and the swelling rate of the modified elastomer is greatly improved. The change in the swelling rate is due to the cross-linking density of the B-PDMS elastomer that is lower than that of the PDMS elastomer, which leads to better flexibility of the elastomer, which plays a positive role in enhancing the stretchability and adhesion of the elastomer. In order to further verify the modification mechanism, we carried out Fourier transform infrared (FT-IR) spectroscopy and differential scanning calorimetry (DSC) characterization of PDMS and B-PDMS. FT-IR spectroscopy was used to characterize B-PDMS prepolymers (before cross-linking) and B-PDMS elastomers (after cross-linking) to confirm that the polymer had been cross-linked, and the results are shown in Figure 2e, f. It can be seen that the polymer has a Si−H group stretching vibration peak (2165 cm^{-1}) before cross-linking, and this characteristic peak basically disappears after cross-linking, indicating that B-PDMS has completed cross-linking.[50,51] This is due to the hydrogenation addition reaction between Si−H and $-CH{=}{=}CH_2$, and the cross-linking reaction consumes the Si−H groups.[38] DSC was employed to characterize the B-PDMS elastomer and the PDMS elastomer. The glass transition temperature of PDMS is −125 °C,[51] and the glass transition temperature of B-PDMS is measured to be −109 °C. It can be seen that the glass transition temperature of the modified PDMS becomes higher. The difference in glass transition temperature between PDMS and B-PDMS can be attributed to the inhibited segmental motion of polymer chains, which is inhibited by Brij during the curing process of PDMS, which results in increased glass transition temperature.[52,53] This verified the inhibitory effect of Brij on the curing process of PDMS.

Stretchability and Flexibility of B-PDMS Elastomers. There are significant differences in flexibility and stretching properties of B-PDMS elastomers prepared under different conditions. We used the Linkam TST350 tensile test bench to test the ultimate strain and elastic modulus of the elastomer. The original state and the stretched state of the elastomer are shown in Figure 3a. We studied Young's modulus and the elongation at break of the B-PDMS elastomer prepared at different curing temperatures and Brij contents; the relationship between stress and strain is shown in Figure 3b. It can be seen that the ultimate strain and the elastic modulus of the B-PDMS elastomer are affected not only by the Brij content and the curing temperature but also by the curing rate. When B-PDMS is cured at a lower temperature, the curing time is significantly prolonged, even a tiny amount of Brij will significantly affect the tensile properties and flexibility of PDMS elastomers. The ultimate strain of an ordinary PDMS elastomer is up to 200% and Young's modulus is up to 4 MPa. The elastomer with better flexibility and higher stretchability can be obtained by adequately increasing the content of Brij and controlling the curing temperature and the curing rate. When 1.2 wt. % Brij was added to PDMS and cured at 50 °C (B3-L-PDMS), the elastomer exhibits the best stretchability, the maximum strain can reach 450%, the stretching effect is far better than that of ordinary PDMS, the Young's modulus is about 0.03 MPa, and the elastomer has outstanding flexibility. Movie S1 (Supporting Information) shows the manual stretch release process of the elastomer. In this work, the curing rate can be better influenced by adjusting the content of Brij in PDMS at a lower curing temperature, and a softer elastomer can be obtained.

Adhesion of the B-PDMS Elastomer. Brij will not only affect the stretching and flexibility of PDMS but also could greatly enhance the adhesion of elastomers. We use tension testing machines to test the adhesion of elastomers. The elastomer is prepared into a square film, its upper and lower surfaces were connected to the skin and the testing machine, respectively,[10] as shown in Figure 3c, and the elastomer has high adhesion to the skin. The adhesion test results of elastomers are shown in Figure 3d. It can be seen that the adhesion of the elastomer is also affected by the Brij content, the curing temperature, and the curing rate, and the adhesion of the elastomer is significantly enhanced even with the addition of a small amount of Brij. When 1.2 wt. % Brij is added to PDMS and cured at 50 °C, the elastomer exhibits the best adhesion, and the maximum adhesion strength can reach 9 kPa, which is not available in ordinary PDMS elastomers. In addition, B-PDMS elastomers also show good adhesion to metal, glass, and polyethylene terephthalate (PET) materials. By placing a layer of B-PDMS film between two glass sheets for the lap shear test, the lap shear strength of B-PDMS elastomers cured at 50 °C was tested, as shown in Figure 3e. The lap shear test can provide information about the adhesion of the sample to the substrate. The lap shear result is related to the flow resistance of the sample and depends on the bond strength of the sample.[34] Figure 3f shows the load−displacement curve of the lap shear test. It can be seen that the higher the content of Brij added in PDMS, the stronger the adhesion of elastomers, resulting in higher lap shear strength. The lap shear strength of B-PDMS elastomers can reach up to 51 N. However, when 2 wt. % Brij is added to PDMS, excessive Brij makes it difficult for PDMS to be effectively cross-linked, leading to a significant reduction in the adhesive strength of elastomers, and hence, the bond failure occurs in the lap shear test.

PDMS is a commonly used biomaterial, and PDMS-based elastomers are often used to contact the human skin. In order to test whether the developed B-PDMS elastomer irritates the skin, the elastomer was attached to the human skin and peeled off after 7 days, and the effect on the skin was observed. As shown in Figure S2 (Supporting Information), there is no irritant reaction such as redness, swelling, or itching on the skin, and there is no residue on the skin. Elastomers can be easily attached to the human skin and can be easily peeled off. In order to test the durability and reusability of the B-PDMS elastomer, we put them in different harsh environments to test their mechanical properties. In order to check whether the elastomer is washable or not, the elastomers were soaked and washed in solvents such as deionized water and ethylene glycol, respectively, and the changes in adhesion force were measured. As shown in Figure S3 (Supporting Information), after washing and drying, the adhesion of the elastomer has no significant change compared with the initial adhesion. In order to test the reusability of the elastomer, the cyclic tensile test was carried out using a horizontal pulling force test machine, and the elastomer was stretched 300 times under the condition of strain 200%. As shown in Figure S4 (Supporting Information), the elastomer can still maintain a limit strain of 400% after several stretches.

https://doi.org/10.1021/acsomega.1c05789
ACS Omega 2022, 7, 5825−5835

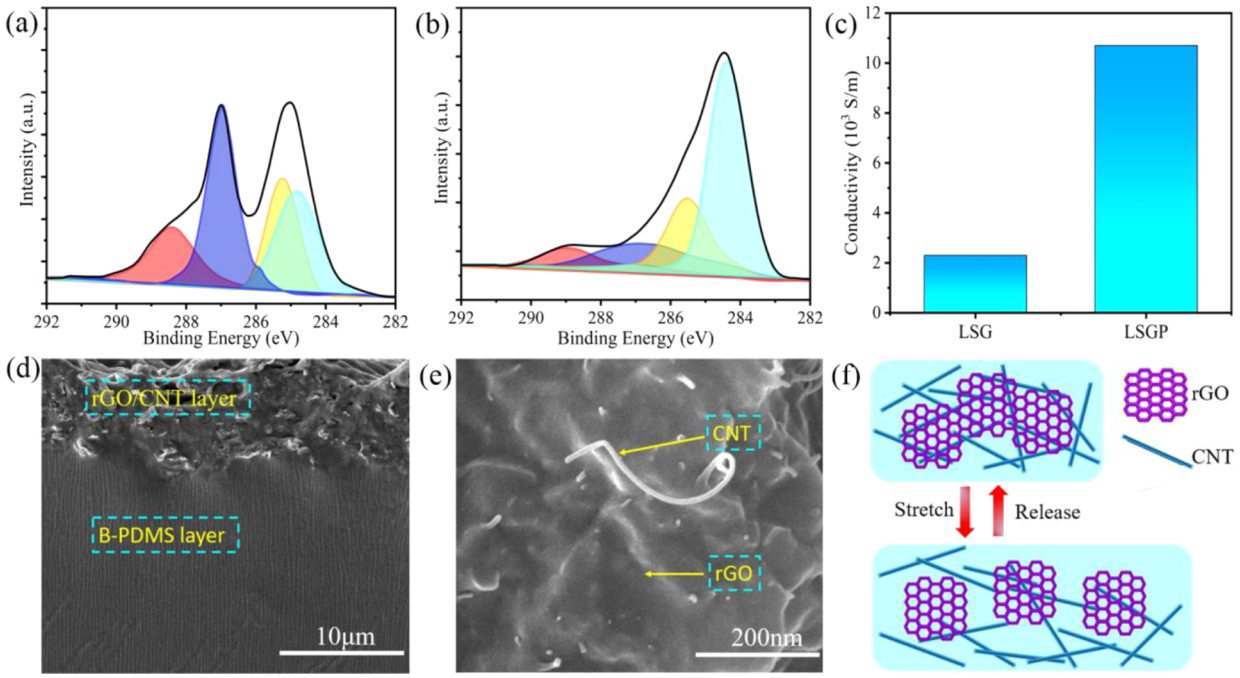

Figure 4. (a) XPS of GO. (b) XPS of rGO powder prepared based on LSG. (c) Conductivity of rGO prepared on GO thin film and the conductivity of the LSGP conductive layer. (d) SEM image of the conductive layer embedded in the adhesive layer. (e) SEM image of the conductive layer with the rGO/CNT ratio of 2:1. (f) Network structure of the conductive layer in the original state and the strain state.

In conclusion, we have prepared a highly stretchable self-adhesive elastomer with adjustable mechanical properties using a highly extensible PDMS modification method. Adding a small amount of Brij-35 to PDMS can change the mechanical properties of PDMS, such as ultimate strain, Young's modulus, and adhesion. When the cross-linking reaction of PDMS is inhibited, it contributes to the formation of heterogeneous cross-linking networks, and the slower curing rate causes the polymer chain to disentangle and thus rearrange the polymer chain. It is worth noting that this is the first study of using Brij to change the mechanical properties of PDMS. The experimental results show that when 1.2 wt. % Brij is added to PDMS and cured at 50 °C, the elastomer has the best flexibility, stretchability, and adhesion, so it can be used as the adhesion layer of the strain sensor to form a good conformation contact between the elastomer and the skin.

2.2. B-PDMS/rGO/CNT Strain Sensor. *Characterization of LSGP.* LSGP is achieved by laser-scribing GO films using the LightScribe DVD burner. When GO is reduced with a DVD burner, the infrared laser of the burner will output a laser of 780 nm so that the GO film will have a photothermal effect in the process of laser-scribing. GO absorbs high-intensity light, photothermal reaction removes most oxygen-containing groups and reduces the carbon content combined with oxygen. After effective photothermal reduction of GO, high-quality rGO was obtained.[54,55] GO and LSGP were characterized by XPS, as shown in Figure 4a, b. Four different peaks were detected in the XPS spectrum, corresponding to C=C/C−C (aromatic ring), C−O (epoxy and alkoxy), C=O (hydroxyl), and C(*O*)O (carboxyl). The intensities of all the peaks of carbon−oxygen binding in rGO were significantly decreased in XPS spectra. This is a typical feature of the effective reduction of GO.[56−58] LSGP is different from the laser-scribed graphene prepared by Kady et al.[37] on the GO film, we peel LSG from the GO film to make it have more flexible applications, and LSGP can be combined with a variety of substances like rGO prepared using a chemical process and is widely used in supercapacitors, strain sensors, and other fields. Moreover, compared with the complex, toxic, and expensive chemical reduction GO process,[35] LSGP is prepared under low-cost, safety, and convenience conditions.

Performance Evaluation of LSGP. The rGO powder prepared based on safe and reliable laser-scribed technology has excellent conductivity and high sensitivity and exhibits the performance required for the synthesis of strain sensors. In order to understand the electrical properties of LSGP, we first compared the conductivity of LSGP and tested the sensitivity in subsequent experiments. First, LSGP powder is prepared into a uniform dispersion, spray-coated on the PET substrate, and dried at room temperature to form a uniform conductive layer. The four-probe method measured the electrical conductivity, and the measurement results are shown in Figure 4c. The conductivity of rGO on the GO film is 2.3×10^3 S/m, the highest conductivity of LSGP can reach 10.7×10^3 S/m, and the electrical conductivity of LSGP increases significantly. The difference in conductivity is attributed to the different densities of rGO in the conductive layer. Because of its higher conductivity and more flexible application, LSGP can be used as a conductive material for sensors and other fields such as supercapacitors, which simplifies the manufacturing process and produces more cost-effective strain sensors.

LSGP and CNT Endow the B-PDMS Elastomer with Electrical Properties. Using the B-PDMS elastomer as the adhesive layer of a strain sensor, the conductive layer can be firmly embedded in the adhesion layer because of the high adhesion of the elastomer, and the conductive layer will not separate or fall off from the adhesive layer even in significant motion.[59] The conductive layer was characterized by scanning electron microscopy (SEM),[37,59,60] as shown in Figure 4d, e. The microscopic morphology of rGO and CNT can be seen

https://doi.org/10.1021/acsomega.1c05789
ACS Omega 2022, 7, 5825−5835

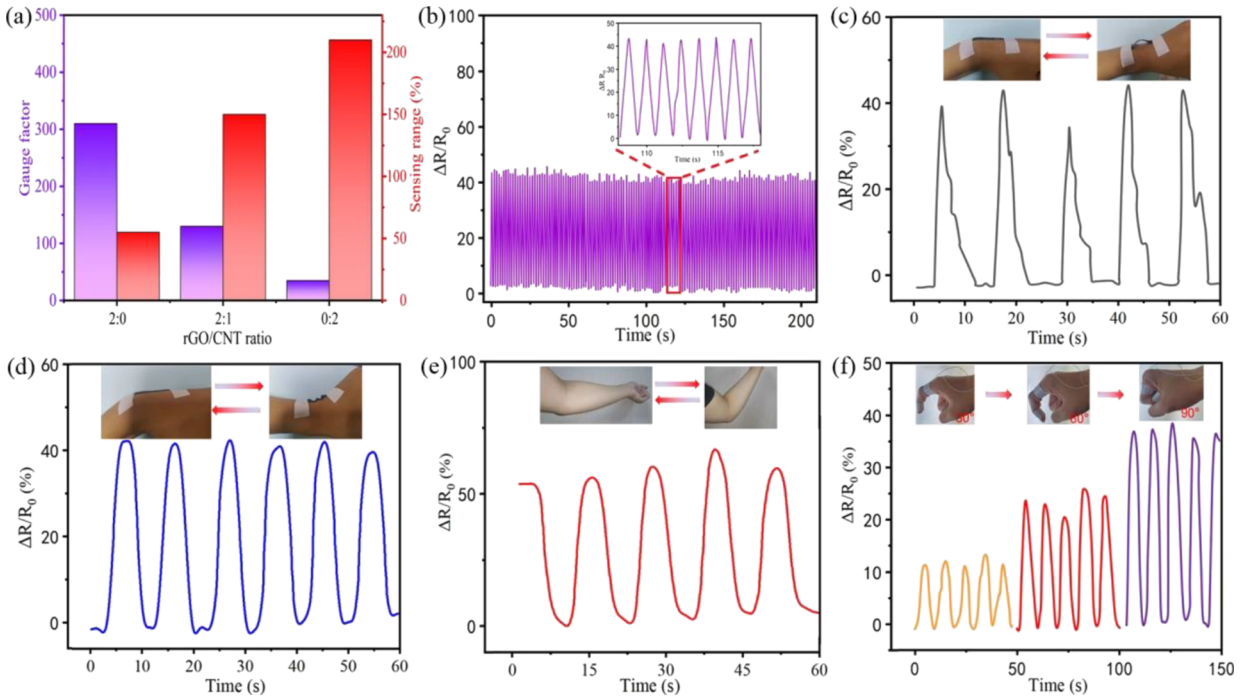

Figure 5. (a) Sensitivity and the sensing range of strain sensors with different rGO/CNT ratios. (b) Periodic change in the relative resistance of the B-PDMS/rGO/CNT strain sensor in the cyclic tensile test. (c) Nonviscous strain sensors monitor wrist bending. (d) Adhesive strain sensor monitors wrist bending. (e) Adhesive strain sensor monitors the strain response of the finger at different degrees of bending. (f) Adhesive strain sensors monitor elbow bending.

clearly by SEM, and the conductive layer is firmly embedded in the B-PDMS elastomer. The thickness of the conductive layer is about 1.5 μm. In order to obtain an elastomer with high sensitivity and a wide detection range, we use both rGO and CNTs as the conductive networks, and the resistance change of the conductive layer is related to the strain. If only a CNT is used, the sensor can have a wide detection range, but the resistance varies little with strain. If only rGO is used, the sensor can have high sensitivity, but the sensing range is small. The conductive network is constructed using the synergistic effect of rGO and CNT so that the elastomer has excellent electrical properties in sensitivity and the dynamic range; rGO acts as a bridge to connect broken CNT networks during tension,[29−31] as shown in Figure 4f.

Performance of the Strain Sensor. The gauge factor (GF) was employed to measure the sensitivity, GF = $(\Delta R/R_0)/\varepsilon$, where $\Delta R/R_0$ represents the relative resistance of the sensor, ε represents the strain range, and R_0 represents the initial resistance of the sensor.[9,34] Strain sensors with different rGO/CNT ratios have different sensitivity and sensing ranges, as shown in Figure 5a. The higher the rGO/CNT ratio, the greater the relative resistance of the strain sensor under the same strain. When the rGO/CNTs ratio is 2:0, the sensor has the highest GF (310) and the lowest sensing range (55%). When the rGO/CNT ratio is 0:2, the sensor has the widest sensing range (210%) and the lowest GF (35). When the rGO/CNT ratio is 2:1, the strain sensor's GF can reach 130, and the sensing range can reach 150%. A strain sensor with an rGO/CNT ratio of 2:1 was selected to monitor human motion. As a wearable device, the flexible strain sensor should not only have an appropriate sensitivity and a sensing range but also maintain good stability in the periodic tension release cycle. In order to test the stability and the durability of the strain sensor, we conducted a tensile release cycle test. As shown in Figure 5b, the relative resistance can remain stable when the sensor is maintained at 60% strain, and the sensor has a good dynamic response.

Joint movements such as fingers, shoulders, and knees are affected by aging, injury, and disease,[34] and monitoring these movements are essential for medical rehabilitation. However, the skin surface is not smooth, the surface of the skin changes irregularly during exercise, and the signals collected using nonadhesive sensors usually contain both artifacts and fault signals. Figure 5c shows the response of a nonadhesive sensor mounted on the wrist, the peak value changes randomly, and significant noise can be observed. Figure 5d shows the response of the adhesive sensor to wrist bending, recording a smooth curve. The high signal quality produced by the adhesive strain sensor can be attributed to its conformal contact with the skin because of the excellent sensing performance of the adhesive sensor and its change in the relative resistance of the strain sensor caused by different motions. As shown in Figure 5e, f, in addition to wrist bending, finger bending (Figure 5e) and elbow bending (Figure 5f) were also measured. $\Delta R/R_0$ changes periodically with the bending of fingers, wrists, and elbows. These results indicate that the B-PDMS/rGO/CNT strain sensor can adhere to the skin to form a good conformation contact, and the sensor has a wide detection range, high sensitivity, excellent stability, and fast response, which has great potential in the fields of medical rehabilitation, intelligent robotics, human-computer interaction.

Applications of the Strain Sensor. The strain sensor based on B-PDMS can monitor human activity accurately and stably. In order to highlight the advantages of the strain sensor based on B-PDMS and get closer to the practical application, we designed a real-time wireless robotic hand control system,[61−63] which is shown in Figure 6a. Combined with the self-designed

https://doi.org/10.1021/acsomega.1c05789
ACS Omega 2022, 7, 5825−5835

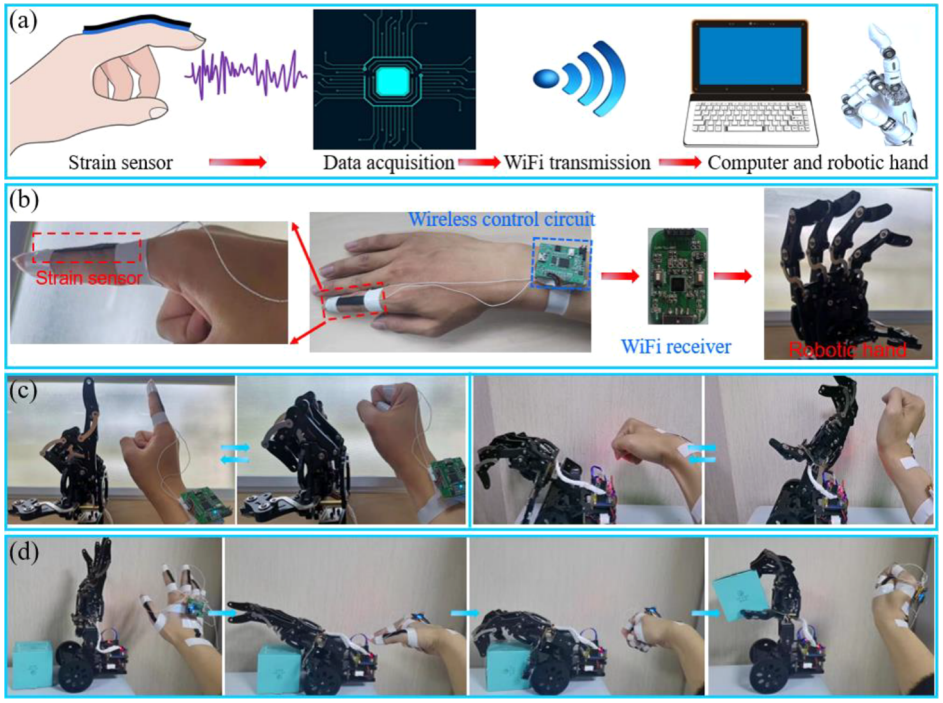

Figure 6. Real-time wireless robotic hand control system: (a) control system schematic diagram, the strain sensor controls the robotic hand through WiFi. (b) Photographs of the control system. (c) Single sensor controls the robotic hand. (d) Multiple sensors control the robotic hand to grasp objects.

circuit, the system can process and transmit strain sensor signals. The physical figure of the robotic hand controlled by the strain sensor through WiFi is shown in Figure 6b. The wireless control circuit is divided into the sending end and the receiving end, and the structural design diagram is shown in Figure S5 (Supporting Information). The sender is connected with the strain sensor as a wearable device, and the receiver is connected with the robotic hand. The transmitter takes the STM32 microcontroller unit as the core, collects the response signal of the strain sensor to the finger bending, converts the resistance change into a digital signal, transmits the signal to the receiver through the wireless WiFi, and converts it into the signal to control the robotic hand. The experiment results show that the circuit we designed based on STM32 is better than the Arduino circuit obviously,[56] and the signal transmission through WiFi is more efficient than the signal transmission through Bluetooth. We control the state of the manipulator by attaching the sensor to the human index finger and wrist and grasp the object through the manipulator, as shown in Figure 6c, d and Movie S2 (Supporting Information). The experimental results show the real-time response of the manipulator to the sensor, and the bending state of the joint corresponds to the position of the manipulator, and the manipulator can accurately reconstruct joint movements and accurately follow the movements of the hand. These results show that combined with some corresponding hardware and software, the strain sensor based on the B-PDMS elastomer has great potential in the fields of robotics, medical rehabilitation, and motion capture.

3. CONCLUSIONS

In conclusion, we innovatively designed a novel and low-cost PDMS modification method, prepared B-PDMS elastomers with excellent mechanical properties by Brij for the first time, and studied the reaction mechanism of Brij-35 that affects PDMS cross-linking. The experimental results show that by controlling the Brij content, curing temperature, and curing time, the stretchability, flexibility, and adhesion of the elastomer can be adjusted. The rearranged polymer chains make the ultimate strain of the B-PDMS elastomer as high as 450%, and the adhesion to the human skin can reach 9 kPa, which is conducive to the conformal adhesion of flexible electronic products. In order to popularize the application of B-PDMS elastomers under safe and convenient conditions, the elastomer is endowed with excellent electrical properties through LSGP and CNTs. The sensor can adhere to the human skin to generate high-quality signals and drive the manipulator through a self-designed real-time wireless control system. We believe that the modification mechanism of Brij on PDMS is helpful for others to further explain the experimental phenomena in practical operation, and our designed flexible materials and general preparation methods can further promote the promotion and application of flexible electronic products when other researchers need to use compliant materials in the fields of skin sensors, friction nanogenerators, supercapacitors, and biomedical adhesives.

4. EXPERIMENTAL SECTION

4.1. Materials. GO (2 mg/mL) dispersion in water was purchased from XFNANO Materials Tech CO., Ltd. (Nanjing, China). CNTs (with a mean diameter of 10−20 nm and a length of 10−30 μm) were obtained from XFNANO Materials Tech CO., Ltd. (Nanjing, China). PDMS (Sylgard 184 silicone elastomer, Dow Corning Corp., USA) consists of a base and a cross-linking agent. Polyoxyethylene lauryl ether (Brij-35) was purchased from BIOISCO Biotechnology Co., Ltd. (Jiangsu Lianyungang). All reagents can be used directly without further purification. The following experimental devices were also

https://doi.org/10.1021/acsomega.1c05789
ACS Omega 2022, 7, 5825−5835

used, including an ultrasonic cell crusher (JY99-IIDN, Ningbo Xinzhi Biotechnology Co., LTD, China), ultrasonic cleaning bath (model UC-4180 L, Shenyang Kewell Experimental Instrument CO., Ltd), and a LightScribe DVD burner (780 nm wavelength and 5 mW output power, infrared laser from the DVD unit).

4.2. Methods. *4.2.1. Preparation of the B-PDMS Elastomer.* Elastomers are prepared by introducing a small amount of Brij-35 in the cross-linking process of PDMS, compared with the elastomers prepared with PDMS barely, and the mechanical properties and the reaction mechanism of B-PDMS are quite different. The default ratio of the PDMS base to the crosslinker is 10:1, adding 8 mg, 16 mg, and 24 mg of Brij-35 to 2 g of PDMS, respectively. The mixture of the PDMS base, the cross-linking agent, and Brij-35 was stirred for 20 min. It should be noted that the mixture needs to be thoroughly stirred so that the Brij is uniformly suspended in the PDMS prepolymer. The mixture was coated on the PET substrate and placed in a vacuum drying box for curing at 50 °C or 100 °C. With the increase in the Brij-35 content, B-PDMS needs a longer curing time at the same temperature. Finally, the B-PDMS elastomer with a thickness of about 0.3 mm is obtained.

4.2.2. Preparation of LSGP. LSGP is achieved by laser-scribing GO films using the infrared laser in the LightScribe DVD burner, and golden-brown GO is converted to black rGO using the photothermal effect. In short, the GO dispersion droplets of about 10 mL were coated on the surface of the LightScribeDVD optical disc, and a layer of GO film was obtained after drying at room temperature. After that, the GO-coated DVD disk was laser-scratched using a LightScribe DVD burner so that the GO was reduced to rGO by the photothermal effect. Then, rGO is stripped from the disc to obtain rGO powder (LSGP). Finally, 50 mg of rGO was mixed with isopropanol of 10 mL, and the mixture was subjected to bath sonication for 1 h and tip sonication for 0.5 h to obtain a uniform rGO dispersion (0.5 wt. %).

4.2.3. Preparation of the B-PDMS/rGO/CNT Strain Sensor. First, 10 mg of CNT was mixed with 10 mL of isopropanol, and the mixture was evenly dispersed by bath ultrasound and tip ultrasound to obtain CNT dispersion (0.1 wt. %). CNT dispersion and rGO dispersion with different volume ratios were mixed, and a uniform rGO-CNT dispersion was obtained after ultrasound. The electrical properties of the conductive layer can be adjusted by adjusting the mixing ratio of CNTs and rGO. Then, the uncured B-PDMS prepolymer was coated on the PET substrate and cured in a vacuum drying oven. Finally, the mixed dispersion was sprayed on the elastomer, and the conductive layer can be attached to the elastomer with high adhesion after drying; the B-PDMS/rGO/CNT strain sensor with an adhesive layer and a conductive layer was obtained.

4.3. Characterization. The ultimate strain and the elastic modulus of the B-PDMS elastomer were measured at the speed of 0.2 mm/s using the Linkam TST350 tensile test bench. The lap shear test and the adhesion test were conducted using the tensile testing machine, the lap shear strength of the sample was measured by placing a B-PDMS film between two glass sheets, and the adhesion was measured by connecting the upper and lower surfaces of the elastomer to the skin and the dynamometer, respectively. FT-IR spectroscopy was used to characterize B-PDMS before and after cross-linking. PDMS before and after modification was characterized by DSC. The content of oxygen-containing functional groups in GO and rGO was measured by X-ray photoelectron spectroscopy (XPS). The structure and morphology of the conductive layer were observed by scanning electron microscopy (SEM). The electrical conductivity of rGO was measured using the four-probe method (Keithley 2420I-V) at room temperature.

■ ASSOCIATED CONTENT

Supporting Information

The Supporting Information is available free of charge at https://pubs.acs.org/doi/10.1021/acsomega.1c05789.

Swelling ratio of H-PDMS elastomers and B3-L-PDMS elastomers, elastomer adheres to the skin for a long time, durability and reusability testing, and wireless control circuit structure diagram (PDF)

Movie S1, manual stretch release process of elastomers (MP4)

Movie S2, the robotic hand is controlled using the B-PDMS/rGO/CNT strain sensor (MP4)

■ AUTHOR INFORMATION

Corresponding Authors

Bin Dong − *College of Electronic Information Engineering & Hebei Key Laboratory of Digital Medical Engineering and Affiliated hospital of Hebei University, Hebei University, Baoding 071000, P. R. China*; Email: Dbin2000@163.com

Xiuling Liu − *College of Electronic Information Engineering & Hebei Key Laboratory of Digital Medical Engineering, Hebei University, Baoding 071000, P. R. China*; Email: liuxiuling121@hotmail.com

Authors

Cunguang Lou − *College of Electronic Information Engineering & Hebei Key Laboratory of Digital Medical Engineering, Hebei University, Baoding 071000, P. R. China*; orcid.org/0000-0001-6019-8125

Enjie Liu − *College of Electronic Information Engineering & Hebei Key Laboratory of Digital Medical Engineering, Hebei University, Baoding 071000, P. R. China*; orcid.org/0000-0002-1637-0116

Tong Cheng − *College of Electronic Information Engineering & Hebei Key Laboratory of Digital Medical Engineering, Hebei University, Baoding 071000, P. R. China*

Jun Li − *College of Electronic Information Engineering & Hebei Key Laboratory of Digital Medical Engineering, Hebei University, Baoding 071000, P. R. China*

Hongzan Song − *College of Chemistry & Environmental Science, Hebei University, Baoding 071000, P. R. China*; orcid.org/0000-0003-3112-2361

Guangwei Fan − *College of Electronic Information Engineering & Hebei Key Laboratory of Digital Medical Engineering, Hebei University, Baoding 071000, P. R. China*

Lei Huang − *Department of Molecular, Cell and Cancer Biology, University of Massachusetts Medical School, Worcester, Massachusetts 01605, United States*

Complete contact information is available at: https://pubs.acs.org/10.1021/acsomega.1c05789

Author Contributions

[⊥]E.L. and C.L. contributed equally to this work.

https://doi.org/10.1021/acsomega.1c05789
ACS Omega 2022, 7, 5825−5835

Notes

The authors declare no competing financial interest.

■ ACKNOWLEDGMENTS

The authors acknowledge the Natural Science Foundation of Hebei Province (F2021201005, F2021201002), the Hebei Province Postdoctoral Scientific Research Project (B2019005001), and the Key Projects of Education Department of Hebei Province (ZD2020146).

■ REFERENCES

(1) Kang, J.; Son, D.; Wang, G. N.; Liu, Y.; Lopez, J.; Kim, Y.; Oh, J. Y.; Katsumata, T.; Mun, J.; Lee, Y.; Jin, L.; Tok, J. B.; Bao, Z. Tough and Water-Insensitive Self-Healing Elastomer for Robust Electronic Skin. *Adv. Mater.* **2018**, *30*, No. e1706846.

(2) Tang, X.; Wu, C.; Gan, L.; Zhang, T.; Zhou, T.; Huang, J.; Wang, H.; Xie, C.; Zeng, D. Multilevel Microstructured Flexible Pressure Sensors with Ultrahigh Sensitivity and Ultrawide Pressure Range for Versatile Electronic Skins. *Small* **2019**, *15*, No. e1804559.

(3) Kim, J.; Lee, M.; Shim, H. J.; Ghaffari, R.; Cho, H. R.; Son, D.; Jung, Y. H.; Soh, M.; Choi, C.; Jung, S.; Chu, K.; Jeon, D.; Lee, S. T.; Kim, J. H.; Choi, S. H.; Hyeon, T.; Kim, D. H. Stretchable silicon nanoribbon electronics for skin prosthesis. *Nat. Commun.* **2014**, *5*, 5747.

(4) Won, P.; Park, J. J.; Lee, T.; Ha, I.; Han, S.; Choi, M.; Lee, J.; Hong, S.; Cho, K. J.; Ko, S. H. Stretchable and Transparent Kirigami Conductor of Nanowire Percolation Network for Electronic Skin Applications. *Nano Lett.* **2019**, *19*, 6087−6096.

(5) Yu, Y.; Nassar, J.; Xu, C.; Min, J.; Yang, Y.; Dai, A.; Doshi, R.; Huang, A.; Song, Y.; Gehlhar, R.; Ames, A. D.; Gao, W. Biofuel-powered soft electronic skin with multiplexed and wireless sensing for human-machine interfaces. *Sci. Robot.* **2020**, *5*, No. eaaz7946.

(6) Faliang, H.; Xingyan, Y.; Hao, G.; Yun, Y.; Tian, B.; Weiguo, W.; Wenxi, G.; Xiangyang, L.; Meidan, Y. Stretchable, Biocompatible, and Multifunctional Silk Fibroin-Based Hydrogels toward Wearable Strain/Pressure Sensors and Triboelectric Nanogenerators. *ACS Appl. Mater. Interfaces* **2020**, *5*, 6442−6450.

(7) Liu, M.; Pu, X.; Jiang, C.; Liu, T.; Huang, X.; Chen, L.; Du, C.; Sun, J.; Hu, W.; Wang, Z. L. Large-Area All-Textile Pressure Sensors for Monitoring Human Motion and Physiological Signals. *Adv. Mater.* **2017**, *29*, No. 1703700.

(8) Taehoon, K.; Junyong, P.; Jongmoo, S.; Donghwi, C.; Seokwoo, J. Bioinspired, Highly Stretchable, and Conductive Dry Adhesives Based on 1D−2D Hybrid Carbon Nanocomposites for All-in-One ECG Electrodes. *ACS Nano* **2016**, *4*, 4770−4778.

(9) Dallinger, A.; Keller, K.; Fitzek, H.; Greco, F. Stretchable and Skin-Conformable Conductors Based on Polyurethane/Laser-Induced Graphene. *ACS Appl. Mater. Interfaces* **2020**, *12*, 19855−19865.

(10) Xu, Z.; Chen, L.; Lu, L.; Du, R.; Ma, W.; Cai, Y.; An, X.; Wu, H.; Luo, Q.; Xu, Q.; Zhang, Q.; Jia, X. A Highly-Adhesive and Self-Healing Elastomer for Bio-Interfacial Electrode. *Adv. Funct. Mater.* **2021**, *31*, No. 2006432.

(11) Zhang, L.; Kumar, K. S.; He, H.; Cai, C. J.; He, X.; Gao, H.; Yue, S.; Li, C.; Seet, R. C.; Ren, H.; Ouyang, J. Fully organic compliant dry electrodes self-adhesive to skin for long-term motion-robust epidermal biopotential monitoring. *Nat. Commun.* **2020**, *11*, 4683.

(12) Marc, P. W.; Georgette, B. S.-B.; Patrick, H. PDMS with designer functionalities—Properties, modifications strategies, and applications. *Prog. Polym. Sci.* **2018**, *17*, 30078.

(13) Lu, T.; Finkenauer, L.; Wissman, J.; Majidi, C. Rapid Prototyping for Soft-Matter Electronics. *Adv. Funct. Mater.* **2014**, *24*, 3351−3356.

(14) Wang, Q.; Yu, Y.; Yang, J.; Liu, J. Fast Fabrication of Flexible Functional Circuits Based on Liquid Metal Dual-Trans Printing. *Adv. Mater.* **2015**, *27*, 7109−7116.

(15) Lei, W.; Jing, L. Pressured liquid metal screen printing for rapid manufacture of high resolution electronic patterns. *RSC Adv.* **2015**, *5*, 57686−57691.

(16) Tian, K.; Suo, Z.; Vlassak, J. J. Chemically Coupled Interfacial Adhesion in Multimaterial Printing of Hydrogels and Elastomers. *ACS Appl. Mater. Interfaces* **2020**, *12*, 31002−31009.

(17) Yujin, Y.; Huiling, T.; Dongsheng, W.; Yadong, J.; Zhen, Y.; Yonghao, Z. One-pot preparation and applications of self-healing, self-adhesive PAA-PDMS elastomers. *J. Semicond.* **2019**, *40*, No. 112602.

(18) Lee, B. K.; Ryu, J. H.; Baek, I. B.; Kim, Y.; Jang, W. I.; Kim, S. H.; Yoon, Y. S.; Kim, S. H.; Hong, S. G.; Byun, S.; Yu, H. Y. Silicone-Based Adhesives with Highly Tunable Adhesion Force for Skin-Contact Applications. *Adv. Healthcare Mater.* **2017**, *6*, No. 1700621.

(19) Dong-Dong, Z.; Ying-Bo, R.; Bao-Qing, Z.; Xin, Q.; Guohua, D.; Yongming, C.; Chen-Yang, L. A self-healing PDMS elastomer based on acylhydrazone groups and the role of hydrogen bonds. *Polymer* **2017**, *120*, 189−196.

(20) Jun, C.; Melissa, A. L.; Gregory, N. T.; Alfred, J. C. Mechanical Properties of End-Linked PEG/PDMS Hydrogels. *Macromolecules* **2012**, *15*, 6104−6110.

(21) Yinlei, L.; Deliu, H.; Huawen, H.; Peng, Y.; Xiaoting, L.; Jianhui, H.; Shaozhen, W.; Guangji, L. Preparation and Properties of Polydimethylsiloxane (PDMS)/Polyethylene Glycol (PEG)-Based Amphiphilic Polyurethane Elastomers. *ACS Appl. Energ. Mater.* **2019**, *10*, 4377−4384.

(22) Cheng-Hui, L.; Chao, W.; Christoph, K.; Jing-Lin, Z.; Lihua, J.; Yang, S.; Peng, Z.; Yi, C.; Franziska, L.; Christian, L.; Xiao-Zeng, Y.; Zhenan, B. A highly stretchable autonomous self-healing elastomer. *Nat. Chem.* **2016**, *8*, 618−624.

(23) Jeong, S. H.; Zhang, S.; Hjort, K.; Hilborn, J.; Wu, Z. PDMS-Based Elastomer Tuned Soft, Stretchable, and Sticky for Epidermal Electronics. *Adv. Mater.* **2016**, *28*, 5830−5836.

(24) Cho, Y. J.; Sundaram, H. S.; Weinman, C. J.; Paik, M. Y.; Dimitriou, M. D.; Finlay, J. A.; Callow, M. E.; Callow, J. A.; Kramer, E. J.; Ober, C. K. Triblock Copolymers with Grafted Fluorine-Free, Amphiphilic, Non-Ionic Side Chains for Antifouling and Fouling-Release Applications. *Macromolecules* **2011**, *44*, 4783−4792.

(25) Hojjat, M.; Jasmina, C.-T. Long-term behavior of nonionic surfactant-added PDMS for self-driven microchips. *Microsyst. Technol.* **2012**, *19*, 143−150.

(26) Squillace, O.; Esnault, C.; Pilard, J. F.; Brotons, G. Grafting Commercial Surfactants (Brij, CiEj) and PEG to Electrodes via Aryldiazonium Salts. *ACS Appl. Mater. Interfaces* **2017**, *9*, 42313−42326.

(27) Badal, M. Y.; Margaret, W.; Nghia, C.; Hossein, S.-M.; Harrison, D. J. Protein separation and surfactant control of electroosmotic flow in poly(dimethylsiloxane)-coated capillaries and microchips. *J. Chromatogr. A* **2002**, *947*, 277−286.

(28) Jabbari, M.; Teymoori, F. An insight into effect of micelle-forming surfactants on aqueous solubilization and octanol/water partition coefficient of the drugs gemfibrozil and ibuprofen. *J. Mol. Liq.* **2018**, *262*, 1−7.

(29) Xiaoxu, X.; Hong, H.; Jing, Z.; Junrong, Y.; Yan, W.; Zuming, H. A spirally layered carbon nanotube-graphene/polyurethane composite yarn for highly sensitive and stretchable strain sensor. *Composites, Part A* **2020**, *135*, No. 105932.

(30) Yue, Z.; Erhui, R.; Ang, L.; Ce, C.; Ronghui, G.; Hong, T.; Hongyan, X.; Mi, Z.; Wenfeng, Q.; Xinyuan, W.; Li, L. A porous self-healing hydrogel with an island-bridge structure for strain and pressure sensors. *J. Mater. Chem. B* **2020**, *9*, 719−730.

(31) Shirui, P.; Zhen, P.; Zhu, J.; Jianqiao, S.; Wendong, Z.; Qiang, Z.; Shengbo, S. A highly stretchable strain sensor based on CNT/graphene/fullerene-SEBS. *RSC Adv.* **2020**, *10*, 11225−11232.

(32) Jidong, S.; Xinming, L.; Huanyu, C.; Zhuangjian, L.; Lingyu, Z.; Tingting, Y.; Zhaohe, D.; Zengguang, C.; Enzheng, S.; Long, Y.; Zhong, Z.; Anyuan, C.; Hongwei, Z.; Ying, F. Graphene Reinforced Carbon Nanotube Networks for Wearable Strain Sensors. *Adv. Funct. Mater.* **2016**, *26*, 2078−2084.

https://doi.org/10.1021/acsomega.1c05789
ACS Omega 2022, 7, 5825−5835

(33) Fei, P.; Si-Ming, C.; Yuhan, L.; Zhuchen, T.; Jianglin, Y.; Kun, N.; Han, Y.; Bin, X.; Yibin, R.; Faxiang, Q.; Shu-Hong, Y.; Yanwu, Z. 3D Graphene Films Enable Simultaneously High Sensitivity and Large Stretchability for Strain Sensors. *Adv. Funct. Mater.* **2018**, *28*, No. 1803221.
(34) Wang, S.; Fang, Y.; He, H.; Zhang, L.; Li, C. A.; Ouyang, J. Wearable Stretchable Dry and Self-Adhesive Strain Sensors with Conformal Contact to Skin for High-Quality Motion Monitoring. *Adv. Funct. Mater.* **2021**, *31*, No. 2007495.
(35) Farshad, T.; Mara, B. G.; Karan, S.; Aleksandar, K.; Lu, Y.; Rajan, K.; Fernando, S.; Jayoung, K.; Joshua, W.; Shemaiah, B.; Michelle, M.; Joseph, W. Laser-Induced Graphene Composites for Printed, Stretchable, and Wearable Electronics. *Adv. Mater. Technol.* **2019**, *4*, No. 1900162.
(36) Lin, J.; Peng, Z.; Liu, Y.; Ruiz-Zepeda, F.; Ye, R.; Samuel, E. L.; Yacaman, M. J.; Yakobson, B. I.; Tour, J. M. Laser-induced porous graphene films from commercial polymers. *Nat. Commun.* **2014**, *5*, 5714.
(37) El-Kady, M. F.; Kaner, R. B. Scalable fabrication of high-power graphene micro-supercapacitors for flexible and on-chip energy storage. *Nat. Commun.* **2013**, *4*, 1475.
(38) Simpson, T. R. E.; Parbhoo, B.; Keddie, J. L. The dependence of the rate of crosslinking in poly(dimethyl siloxane) on the thickness of coatings. *Polymer* **2003**, *44*, 4829−4838.
(39) Simpson, T. R. E.; Tabatabaian, Z.; Jeynes, C.; Parbhoo, B.; Keddie, J. L. Influence of interfaces on the rates of crosslinking in poly(dimethyl siloxane) coatings\. *J. Polym. Sci., Part A: Polym. Chem.* **2004**, *42*, 1421−1431.
(40) Piotr, M.; Sindhu, V.; Anne Ladegaard, S. How to tailor flexible silicone elastomers with mechanical integrity: a tutorial review. *Chem. Soc. Rev.* **2019**, *48*, 1448−1464.
(41) Ruslan, Y. L.; Aidar, M. K.; Aleksandr, V. S.; Giyjaz, E. B.; Dmitry, G. Y. Platinum-Catalyzed Hydrosilylation in Polymer Chemistry. *Polymer* **2020**, *12*, 2174.
(42) Toerne, K.; Rogers, R.; von Wandruszka, R. Thermal Stability of Nonionic Surfactant Aggregates. *Langmuir* **2001**, *17*, 6119−6121.
(43) Kim, J. H.; Kim, S. R.; Kil, H. J.; Kim, Y. C.; Park, J. W. Highly Conformable, Transparent Electrodes for Epidermal Electronics. *Nano Lett.* **2018**, *18*, 4531−4540.
(44) Marek, M.; Jacques, W. M. N.; Guy, V. The influence of loose and semianchored siloxane polymer chains on the tack of crosslinked silicone rubber. *J. Appl. Polym. Sci.* **2009**, *114*, 1357−1364.
(45) Huang, J.; Cai, Y.; Xue, C.; Ge, J.; Yu, S. H. Highly stretchable, soft and sticky PDMS elastomer by solvothermal polymerization process. *Nano Res.* **2021**, *28*, 5830−5836.
(46) Li-Heng, C.; Thomas, E. K.; Rodrigo, E. G.; Adrian, F. P.; Michael, R.; David, A. W. Soft Poly(dimethylsiloxane) Elastomers from Architecture-Driven Entanglement Free Design. *Adv. Mater.* **2015**, *27*, 5132−5140.
(47) Schultz, C. W.; Ng, C. L. W.; Yu, H. Z. Superhydrophobic Polydimethylsiloxane via Nanocontact Molding of Solvent Crystallized Polycarbonate: Optimized Fabrication, Mechanistic Investigation, and Application Potential. *ACS Appl. Mater. Interfaces* **2020**, *12*, 3161−3170.
(48) Johnston, I. D.; McCluskey, D. K.; Tan, C. K. L.; Tracey, M. C. Mechanical characterization of bulk Sylgard 184 for microfluidics and microengineering. *J. Micromech. Microeng.* **2014**, *24*, No. 035017.
(49) Lee, J. N.; Park, C.; Whitesides, G. M. Solvent compatibility of poly(dimethylsiloxane)-based microfluidic devices. *Anal. Chem.* **2003**, *75*, 6544−6554.
(50) Carlborg, C. F.; Haraldsson, T.; Cornaglia, M.; Stemme, G.; vander Wijngaart, W. A High-Yield Process for 3-D Large-Scale Integrated Microfluidic Networks in PDMS. *J. Microelectromech. Syst.* **2010**, *19*, 1050−1057.
(51) Rutnakornpituk, M.; Ngamdee, P.; Phinyocheep, P. Synthesis, characterization and properties of chitosan modified with poly-(ethylene glycol)-polydimethylsiloxane amphiphilic block copolymers. *Polymer* **2005**, *46*, 9742−9752.
(52) Imen, A.-M.; Taha, C.; Saber, C.; Houyem, A.; Patrice, S.-M.; Hervé, C.; Catherine, M.; Régis, M.; Hatem Ben, R.; Emmanuelle, V.; Abdelhamid, E.; Nicole, J.-R. Novel PDMS based Semi-Interpenetrating Networks (IPNs) for the extraction of phenolic compounds. *J. Environ. Chem. Eng.* **2020**, *9*, No. 104656.
(53) Sheng, J.; Zhang, M.; Xu, Y.; Yu, J.; Ding, B. Tailoring Water-Resistant and Breathable Performance of Polyacrylonitrile Nanofibrous Membranes Modified by Polydimethylsiloxane. *AACS Appl. Mater. Interfaces* **2016**, *8*, 27218−27226.
(54) Rouzbeh, K.; Kimball, A.; Lazarus, M.; Woo Soo, K. Highly Sensitive Pressure Sensor Array With Photothermally Reduced Graphene Oxide. *IEEE Electron Device Lett.* **2015**, *36*, 180−182.
(55) Petridis, C.; Lin, Y. H.; Savva, K.; Eda, G.; Kymakis, E.; Anthopoulos, T. D.; Stratakis, E. Post-fabrication, in situ laser reduction of graphene oxide devices. *Appl. Phys. Lett.* **2013**, *102*, No. 093115.
(56) Qiang, B.; Yanhu, Z.; Fangfang, H.; Marino, L.; Hesheng, X. Stretchable conductive films based on carbon nanomaterials prepared by spray coating. *J. Appl. Polym. Sci.* **2015**, *133*, 43243.
(57) Zhang, J.; Yang, H.; Shen, G.; Cheng, P.; Zhang, J.; Guo, S. Reduction of graphene oxide via L-ascorbic acid. *Chem. Commun.* **2010**, *46*, 1112−1114.
(58) Yang, G.; Qi, L.; Rongyao, W.; Jin, S.; Yongfeng, L.; Fuzhen, X. Laser Direct Writing of Ultrahigh Sensitive SiC-Based Strain Sensor Arrays on Elastomer toward Electronic Skins. *Adv. Funct. Mater.* **2019**, *29*, No. 1806786.
(59) Junjun, D.; Shichen, F.; Runzhi, Z.; Eric, B.; Woo, L.; Frank, T. F.; Eui-Hyeok, Y. Graphene−Vertically Aligned Carbon Nanotube Hybrid on PDMS as Stretchable Electrodes. *Nanotechnology* **2017**, *28*, 465302.
(60) Yun, C.; Junyu, L.; Shuang, Z.; Dachuang, S.; Yan, H.; Xin, C.; Jian, G.; Ni, Z.; Ching-Ping, W. UV Laser-Induced Polyimide-to-Graphene Conversion: Modeling, Fabrication, and Application. *Small Methods* **2019**, *3*, No. 1900208.
(61) Zhengguang, Y.; Liangliang, W.; Yifan, X.; Rendong, Q.; Wenquan, L.; Min, W.; Yan, Z.; Shunli, Z.; Chunyang, J.; Miaomiao, Z.; Ruirui, C.; Zhaoling, L.; Xin, W. Flexible High-Resolution Triboelectric Sensor Array Based on Patterned Laser-Induced Graphene for Self-Powered Real-Time Tactile Sensing. *Adv. Funct. Mater.* **2021**, *31*, No. 2100709.
(62) Li, C.; Cui, Y. L.; Tian, G. L.; Shu, Y.; Wang, X. F.; Tian, H.; Yang, Y.; Wei, F.; Ren, T. L. Flexible CNT-array double helices Strain Sensor with high stretchability for Motion Capture. *Sci. Rep.* **2015**, *5*, 15554.
(63) Cheng-Zhou, H.; Xue-Feng, Z.; Song-Yan, X.; Ying-Hui, S.; Kai-Ping, Y.; Fan, Y.; Qi-Gang, W.; Jia-Cheng, W.; David Wei, Z.; Hong-Liang, L. Highly stretchable and self-healing strain sensors for motion detection in wireless human-machine interface. *Nano Energy* **2020**, *76*, No. 105064.

https://doi.org/10.1021/acsomega.1c05789
ACS Omega 2022, 7, 5825−5835